

THE CRYSTAL STRUCTURE AND POLY- TYPISM OF MANGANPYROSMALITE

YOSHIO TAKÉUCHI, ISAO KAWADA, SHIGEKO IRIMAZIRI,
and RYOICHI SADANAGA

*Mineralogical Institute, Faculty of Science, University
of Tokyo, Hongo, Tokyo*

ABSTRACT

The crystal structure of manganpyrosmalite has been determined. There are two chemical units of $(\text{Mn, Fe})_8\text{Si}_6\text{O}_{16}(\text{OH, Cl})_{10}$ in the unit cell of symmetry $P3m1$ with $a = 13.42$, $c = 7.159\text{\AA}$. The reciprocal lattice constructed from Weissenberg photographs revealed a marked substructure corresponding to the pyrochroite layer, suggesting that the structure contains the same type of layers. The structure analysis was therefore initiated with this assumption in mind, and a complement structure consisting of Si and O was determined by a partial Patterson synthesis. The structure thus determined revealed that a silicate sheet of a new type is contained, which is composed of 12-, 6- and 4-membered rings of SiO_4 tetrahedra with the ratio of 1:2:3, and the whole structure is built up of layers composite of a pyrochroite-like Mn octahedral sheet and a silicate sheet. Since this structure is the first example of Mn sheet silicates which, owing to the large size of Mn ions, inevitably exhibit considerable misfits between octahedral- and tetrahedral sheets, some details of deformations of these sheets are described.

The structures polytypic of this crystal and having three-fold axes are derived and possible polytypic relations between manganpyrosmalite-pyrosmalite and schallerite-friedelite are discussed.

Introduction

Recent investigations into the detailed structures of layer silicates have revealed that the silicate sheets are more or less deformed from their ideal hexagonal symmetry so as to adapt themselves to the adjoining octahedral sheets. For instance, the characteristic difference in configuration between the tetrahedral sheets in dioctahedral layer

silicates and that of trioctahedral layer silicates has been studied in detail (Takéuchi, 1965a). It is inferred however that if any cations larger than magnesium are contained in a considerable amount in a crystal of this group where tetrahedral cations are mainly silicon, dimensional misfit between the octahedral- and tetrahedral-sheets would become so large that it may not be improved either by rotation or tilting of tetrahedra of the six-membered rings in the silicate sheets. Since, in silicates, manganese is the largest cation that is usually found at the center of a polyhedron close to the regular octahedron, it is highly probable that manganese-bearing layer silicates would have a feature different from other layer silicates.

On the other hand, pyrosmalite is a trigonal mineral having the ideal composition of $(\text{Mn, Fe})_8\text{Si}_6\text{O}_{15}(\text{OH, Cl})_{10}$. Judging from the lattice constants and the space group of this crystal reported by Gossner and Mussgnug (1931), it is strongly suspected if the structure of this mineral is of a new type and presents an example of unreconcilable misfit between the two kinds of sheet discussed above. In order to elucidate this point, the present investigation was undertaken of manganpyrosmalite. Frondel and Bauer (1953) already suggested the possibility of a layer structure for this crystal while McConnell (1954) pointed out that the tetrahedral sheets common in ordinary layer silicates do not fit into the hexagonal cell of this material. A brief account on the crystal structure of manganpyrosmalite was presented by Takéuchi, Kawada and Sadanaga in 1963 and based on this, but using a much poorer crystal which gave only 35 reflections, the structure of pyrosmalite was investigated by Kashaev (1968).

Experimental

Crystals used in this study are from the Kyurazawa mine, Tochigi Prefecture, Japan (Watanabe *et al.* 1957). They are tabular perpendicular to the *c*-axis, 2-3 mm in breadth and about 1 mm in

thickness, pinkish in colour and translucent, and show a perfect basal cleavage. The chemical composition was determined as $(\text{Mn}_{12.42}\text{Fe}_{2.77}\text{Mg}_{0.59})(\text{Si}_{12.38}\text{Al}_{0.21})\text{O}_{30.65}(\text{OH}_{17.46}\text{Cl}_{2.96})$ (Watanabe *et al.* 1961) which is very close to the ideal formula $(\text{Mn, Fe})_8\text{Si}_6\text{O}_{15}(\text{OH, Cl})_{10}$ assigned by Frondel and Bauer (1953).

Weissenberg photographs about the c - and a -axes and precession photographs about the a -axis were taken with $\text{CuK}\alpha$ radiation. Platy specimens, approximately 0.5 mm in breadth and 0.5 mm in thickness, were used. For recording the intensities of reflections, the integrating Weissenberg method was employed with the multiple film technique and was supplemented with the precession method for reflections of low diffraction angles. In each of the a -axis Weissenberg photographs, some of the reflections are associated with weak diffuse streaks parallel to the c^* -axis, indicating the presence of a structural fault. For intensity measurements carried out visually with the aid of intensity wedges, the possible effect of these weak streaks was not taken into account. The relative intensities, corrected for the Lorentz and polarization factors, were put on to an absolute scale successively by comparing $\Sigma|F_o|$ and $\Sigma|F_c|$ at each stage of refinements. No correction for extinction was made. However, corrections for transmission factors were performed according to Burnham's program (Burnham, 1963) modified for HITAC 5020E (Takeda & Irimaziri, 1967) available at the Computing Center of the University of Tokyo.

Unit cell and space group

Manganpyrosmalite is trigonal and the lattice constants of this specimen determined from the powder diffractometer measurements by Watanabe *et al.* (1961) are $a = 13.42 \text{ \AA}$ and $c = 7.159 \text{ \AA}$. These were in excellent agreement with the present single crystal data and adopted throughout the course of this study. There are two formula units of $(\text{Mn, Fe})_8\text{Si}_6\text{O}_{15}(\text{OH, Cl})_{10}$ in the cell.

A test for piezoelectricity was carried out with the method developed by Iitaka (1953) and it was found that the effect was negative. Therefore the crystal class was determined to be trigonal holohedral. No rule of extinction was observed among various sets of reflections, and this fact together with the positions of mirror planes recognized in the intensity distribution of reflections indicated the space group $P3m1$ which is in agreement with the one reported by Gossner and Mussnug (1931).

Structure analysis

At the beginning of the structure analysis, it was inferred that the structure would contain an octahedral layer built up of manganese ions and some of the anions. In fact, if we compare the a -axis of the crystal with that of pyrochroite, $Mn(OH)_2$, we can see that one-fourth of the a -length of the former is very close to the a -length of the latter. Therefore, it was assumed that the structure would bear a pyrochroite-like layer. This assumption was also supported by the intensity distribution over the $hk0$ reciprocal net plane (Fig. 1a) constructed from the c -axis Weissenberg photographs, namely, the reflections with both h and k being $4n$ are always very strong. A Patterson projection on to (001) also revealed a marked substructure corresponding to the structure of pyrochroite, which in turn prevented us to proceed to a straight-forward analysis of the structure from the Patterson function. We further calculated the Fourier transform of an Mn octahedron projected along its trigonal axis, and compared it with the $hk0$ reciprocal net of manganpyrosmalite (Fig. 1a and 1b). As observed in Fig. 1, the strongest reflections correspond to the locations of high peaks in the Fourier transform.

Therefore, in order to determine the structure complement to the pyrochroite part and consisting of Si and O, a Patterson synthesis with coefficients, $|\Delta F_o|^2$ for the reflections with both h and k being $4n$, and $|F_o|^2$ for the other, where $\Delta F_o = F_o - F_c(\text{pyrochroite})$, was

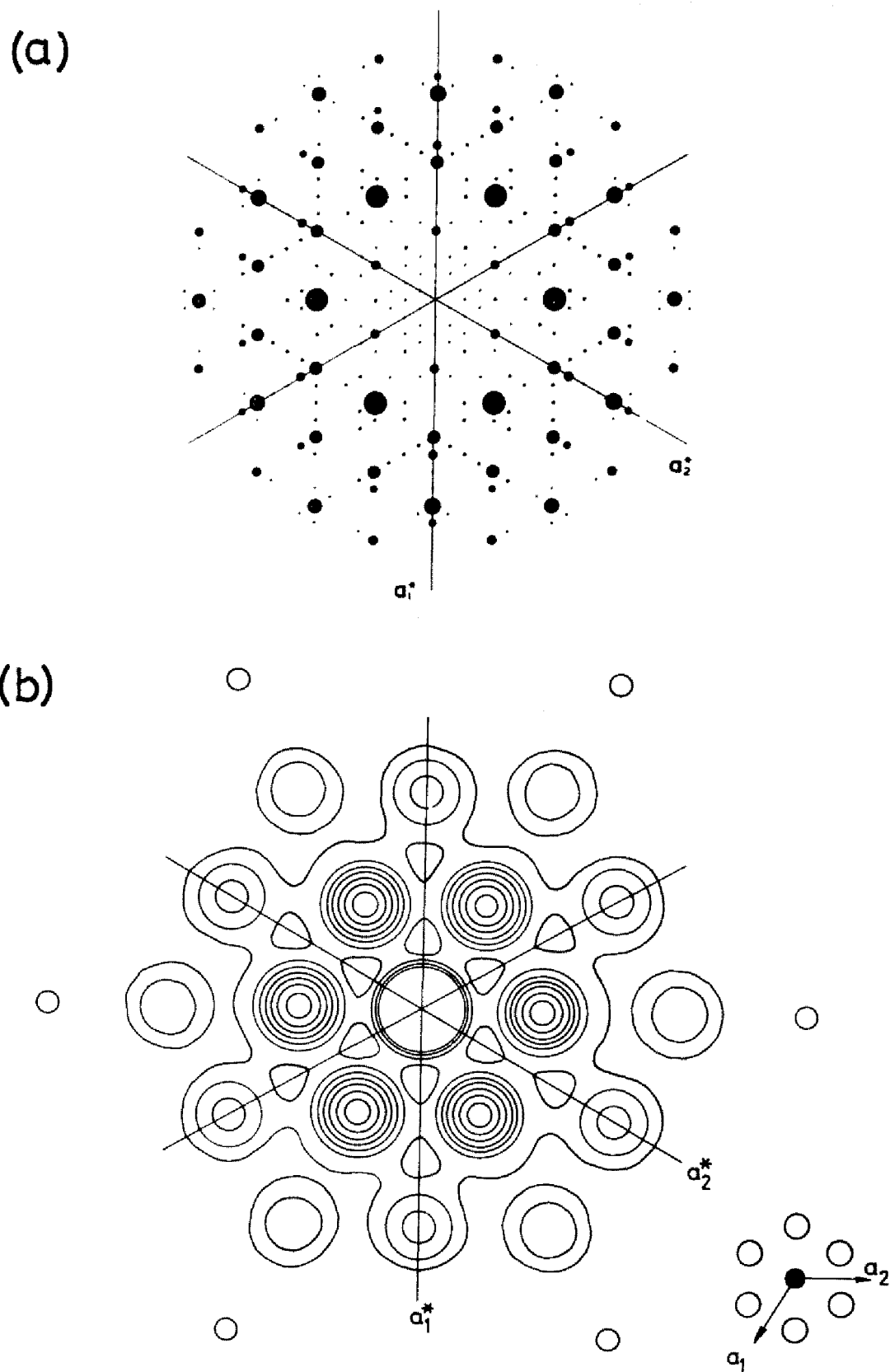


Fig. 1. Comparison of a weighted $hk0$ reciprocal net plane of manganpyrosmalite (a) to the Fourier transform of a manganese-oxygen octahedron projected along its trigonal axis (b). The octahedron is shown on the lower right.

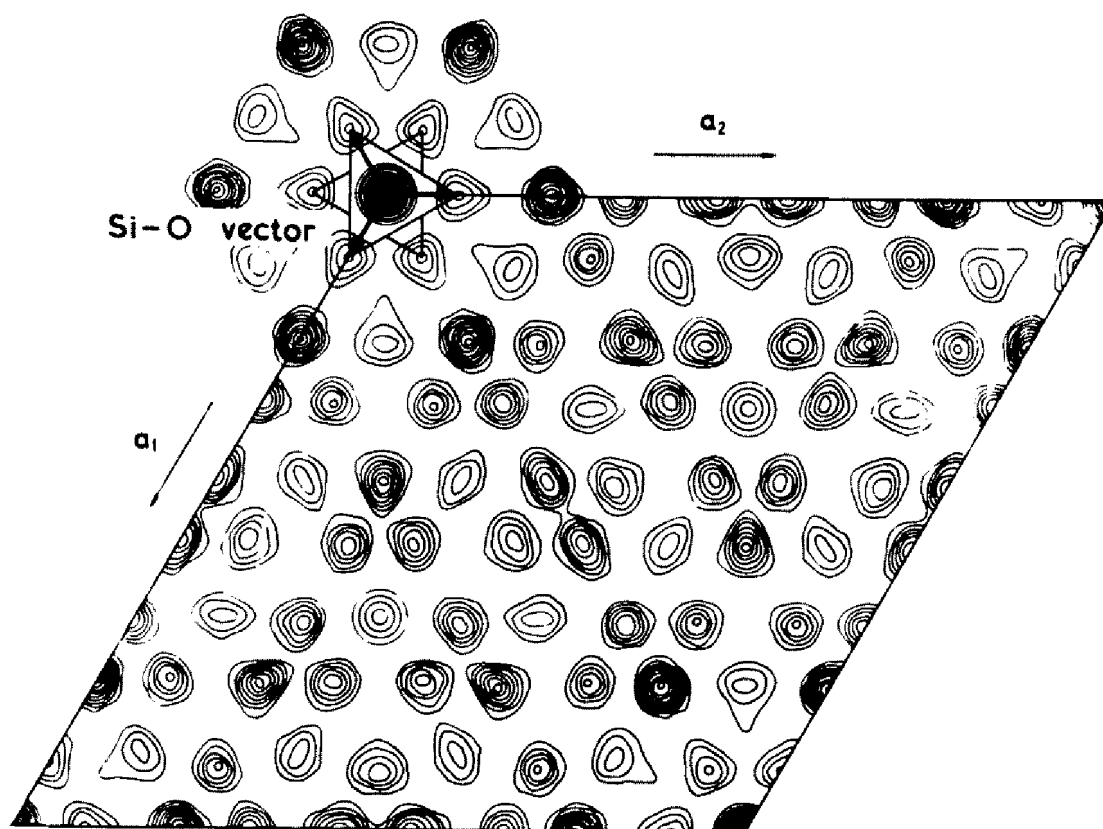


Fig. 2. Patterson projection on (001) with coefficients $|\Delta F|^2(h, k = 4n)$ and $|F_0|^2(h, k \neq 4n)$. Contours at equal but arbitrary intervals. Si-O vectors are indicated.

calculated, where the signs of F_o 's($h, k = 4n$) were taken as the same as those of F_c 's (pyrochroite). Around the origin of the Patterson projection, thus obtained, the peaks corresponding to Si-O vectors were successfully identified (Fig. 2). A salient feature in this map is the array of peaks distributed approximately over the points of a mesh derived by dividing the a_1 - and a_2 - axes equally by nine. This indicates that the atoms in the complement structure nearly lie at some of these points. Then, the orientations of Si-O tetrahedra obtained above as well as the Si:O ratio in the crystal being taken into account, a reasonable linkage of Si-O tetrahedra was deduced as shown in Fig. 3, and by the addition of the pyrochroite layer to it, a probable model of the structure was derived.

The structure thus obtained was refined in the c - and a -axis

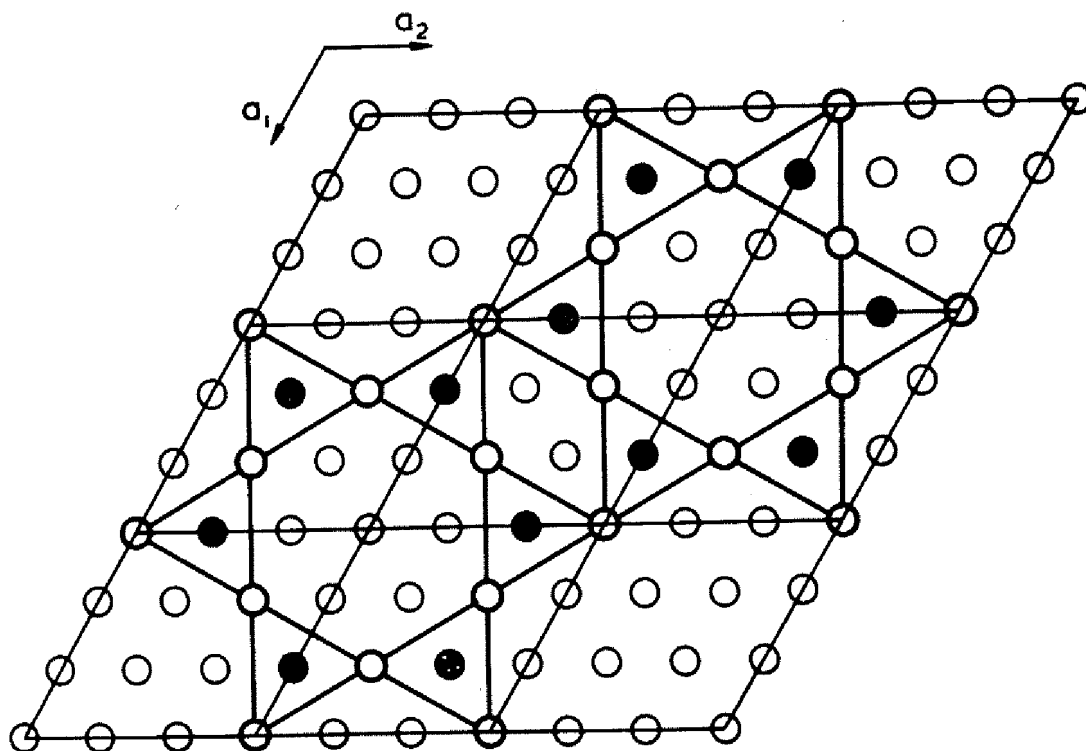


Fig. 3. Reasonable linkage of Si-O tetrahedra. Open and solid circles indicate the approximate peak locations of the Patterson map in Fig. 2.

projections by successive difference syntheses until the disagreement index, R , was reduced to around 30% for both projections. Three-dimensional least-squares refinement was then performed with the full-matrix program, ORFLS, written for IBM 7090 computer by Busing, Martin and Levy (1962) and modified by Iitaka for HITAC 5020E. Undetectable intensities were not included in the calculation of the parameter shifts. Partly ionized form-factors given by Hoerni and Ibers, and Hartree and Hartrees were employed for O and Si respectively, and the ionized form-factor given by Piper for Mn*.

Reflections used for calculations were assigned equal weights at the initial stages of the refinements, and at the final stage the weighting scheme adopted was one for which the product of weight and R was constant for all the values of F_o (Wuensch *et al.* 1966). The

* *International Tables for X-Ray Crystallography* (1962), the Kynoch Press, Birmingham, 202-204.

Table 1. Atomic parameters of manganpyrosmalite

Atom	x	y	z	B
Mn1	0	0	0	3.47 ± 0.24
Mn2	0.2561 ± 0.0002	0	0	1.99 ± 0.07
Mn3	0.5	0	0	2.49 ± 0.10
Mn4	0.5116 ± 0.0005	0.2558	0.0376 ± 0.0006	2.09 ± 0.07
Si	0.4402 ± 0.0003	0.1084 ± 0.0002	0.6213 ± 0.0006	0.92 ± 0.05
O1	0.3294 ± 0.0009	0	0.5	1.88 ± 0.22
O2	0.5670 ± 0.0004	0.1340	0.5535 ± 0.0014	0.19 ± 0.18
O3	0.4295 ± 0.0010	0.2147	0.5776 ± 0.0014	1.12 ± 0.19
O4	0.3939 ± 0.0007	0.0750 ± 0.0008	0.8462 ± 0.0014	1.25 ± 0.13
OH1	0.1806 ± 0.0010	0.0903	0.7733 ± 0.0014	0.71 ± 0.17
OH2	0.3474 ± 0.0010	0.1737	0.1069 ± 0.0017	1.95 ± 0.18
OH3	0.5670 ± 0.0007	0.1340	0.1894 ± 0.0022	3.56 ± 0.33
OH4	0.6667	0.3333	0.7713 ± 0.0074	4.42 ± 1.38

OH groups are partly substituted by Cl.

final R value obtained was 19.8%. In spite of the absorption correction we made, disagreement index could not be reduced further, and this may be ascribed to possible errors in intensities due to the diffuse streaks observed in the Weissenberg photographs and the relatively large size of the specimens we used. However, the value was regarded as small enough to establish the essential feature of the structure. The final atomic parameters are tabulated in Table 1*.

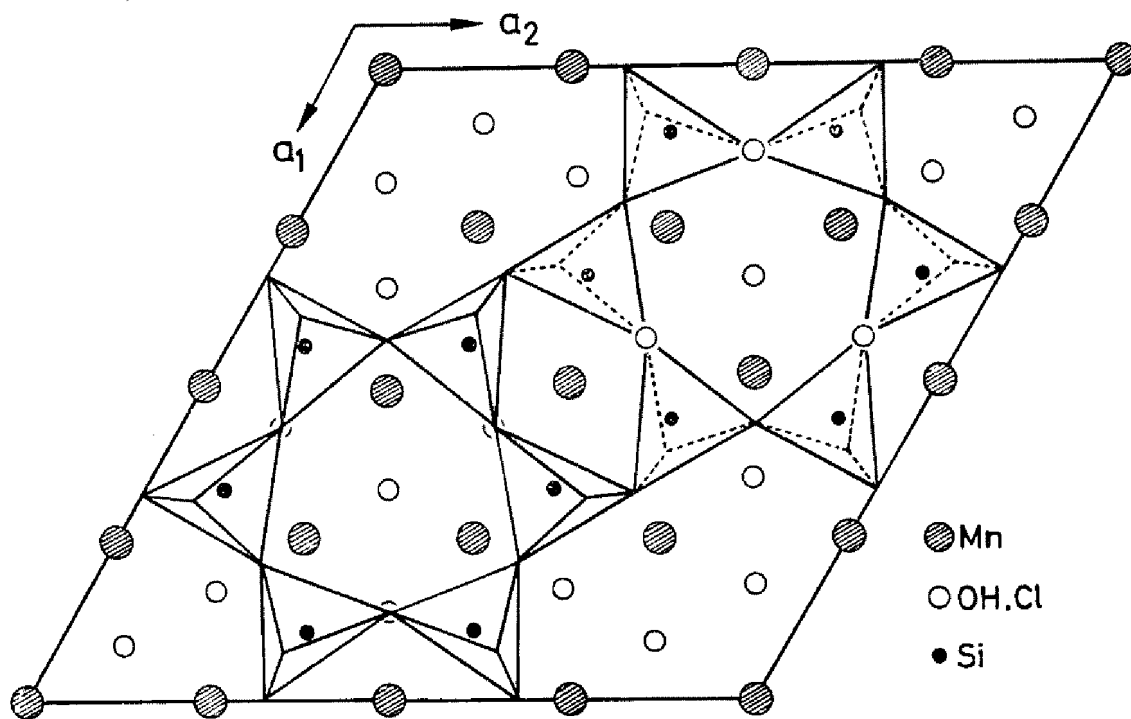


Fig. 4. Crystal structure of manganpyrosmalite projected along the c -axis.

Discussion of the structure

The structure of manganpyrosmalite consists of an octahedral sheet of manganese and a sheet of linked silicon-oxygen tetrahedra. Thus, manganpyrosmalite is a layer silicate but, unlike other layer silicates such as micas and kaolinite, the octahedral sheets are joined

* Table of $|F_o|$ and F_c may be obtained, upon request, from the Mineralogical Institute, Faculty of Science, University of Tokyo, Hongo, Tokyo, Japan.

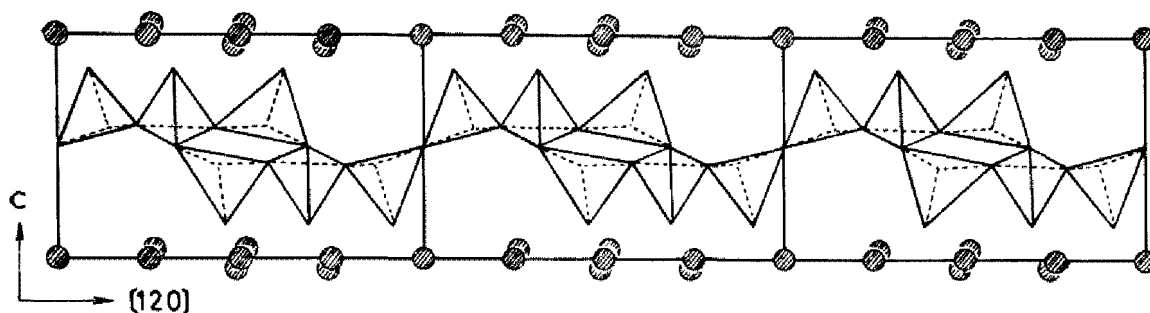


Fig. 5. Projection of a tetrahedral sheet of manganpyrosmalite along the a -axis, indicating the wavy form of the sheet. Three unit cells are shown. OH(Cl) ions are not indicated.

together by silicon tetrahedra. In the tetrahedral sheet which consists of a six-membered ring of linked silicon-oxygen tetrahedra, the apices of a ring point upwards and downwards alternately along the $[210]$ direction as shown in Fig. 4 and 5, and the resulting sheet is as a whole, composed of 12-, 6- and 4- membered rings with the ratio of 1:2:3. The six-membered ring has a trigonal symmetry and the constituent tetrahedra of the ring are considerably tilted from a line perpendicular to the octahedral sheet, the maximum angle between the line and the Si-O apical bonds being about 20° . Such a tilting of tetrahedra can be regarded as an inevitable consequence of misfit between a hexagon formed by the apical oxygens of a tetrahedron and the corresponding oxygen hexagon in the Mn octahedral sheet, the misfit index D (Takéuchi, 1965a) being $+8.8$. The tilting of tetrahedra gives the tetrahedral sheet a wavy appearance as shown in Fig. 5. A similar configuration of a tetrahedral sheet has been reported by Kunze (1956, 1958) in antigorite. For this case the wave is one dimensional and has a long period, while for the case of manganpyrosmalite, the wave is two dimensional and its symmetry is most adequately expressed by the two dimensional Shubnikov symmetry, $p6'mm'$. In comparison with the wave in antigorite, this two-dimensional wave of a shorter periodicity in manganpyrosmalite is evidently caused by its larger D value than

Table 2. Bond lengths, bond angles and interatomic distances in manganpyrosmalite

Si-O1	$1.709 \pm 0.013 \text{ \AA}$	O2-O3	$2.570 \pm 0.013 \text{ \AA}$
Si-O2	1.632 ± 0.007	O3-O1	2.559 ± 0.017
Si-O3	1.537 ± 0.014	O1-O4	2.652 ± 0.015
Si-O4	1.703 ± 0.011	O2-O4	2.929 ± 0.015
O1-O2	2.796 ± 0.013	O3-O4	2.558 ± 0.015
O1-Si-O2	$113.6^\circ \pm 1.1^\circ$	O1-Si-O4	$102.0^\circ \pm 1.0^\circ$
O2-Si-O3	108.4 ± 2.9	O2-Si-O4	122.8 ± 1.2
O3-Si-O1	104.0 ± 2.8	O3-Si-O4	104.2 ± 2.7
Mn1-OH1	$2.653 \pm 0.013 \text{ \AA}$	Mn3-OH3	$2.064 \pm 0.015 \text{ \AA}$
Mn2-OH1	2.521 ± 0.013	Mn4-O4	2.535 ± 0.011
Mn2-OH2	2.160 ± 0.013	Mn4-OH2	1.972 ± 0.014
Mn2-O4	1.945 ± 0.010	Mn4-OH3	2.371 ± 0.012
Mn3-O4	2.385 ± 0.010	Mn4-OH4	2.624 ± 0.030

that of antigorite which is +2.0.

In layer silicates in general, the Si-O tetrahedron is nearly regular, but in manganpyrosmalite it is rather deformed. In Table 2, which shows the bond lengths and bond angles found in manganpyrosmalite, it will be seen that the Si-O bond lengths vary considerably. However, the feature that the average length of the apical edges is longer than that of the basal edges is in common with tetrahedra in other layer silicates (Takéuchi, 1965b). In other words the tetrahedra are slightly elongated along apical bonds, the average length of apical and basal edges being 2.713 \AA and 2.641 \AA respectively. Such a mode of deformation of tetrahedra is also observed in pyroxene structures, in which tetrahedra are connected with octahedral chains so that their apical bonds are nearly perpendicular to the chains. For instance, in johannsenite, MnSiO_3 (Freed and Peacor, 1967), the average values of apical edges and basal edges are respectively 2.713 \AA and 2.645 \AA which are quite similar to those of manganpyrosmalite.

Cl atoms are randomly distributed over the possible OH sites of

the Mn octahedral sheets. Until the final stage of the refinements, we assumed that the two Cl atoms in a cell are located on the discrete sites, $2d$ ($1/3\ 2/3\ z$; $2/3\ 1/3\ z$). However, we found that the isotropic temperature factors of the Cl atoms were as large as about 8. Since this value is considerably larger than the commonly observed ones in silicates, we repeated calculations of least-squares and three-dimensional difference syntheses and carefully examined their z -coordinates with a doubt if the large temperature factor was due to errors in coordinates. However, the results of our calculations unravelled their random distribution over the OH sites. The temperature factor of the atoms at $2d$ sites was then reduced to 4.4.

In the results of the following chemical analyses so far reported for pyrosmalite-manganpyrosmalite, we can observe that the amount of Cl atoms per cell varies from specimen to specimen, showing a tendency of increasing Cl atoms with decreasing OH contents,

	OH	Cl	Total (atom per cell)
manganpyrosmalite ¹⁾ (Sterling Hill)	18.95	2.24	21.20
manganpyrosmalite ²⁾ (Kyurazawa)	17.46	2.96	20.42
pyrosmalite ³⁾ (Kyurazawa)	15.23	3.35	18.58

1) Frondel and Bauer, 1953

2) J. Ito (Watanabe *et al.* 1961)

3) H. Haramura (Watanabe *et al.* 1961)

Moreover, in some of the specimens of friedelite and schallerite which are, as discussed later, closely related to pyrosmalite, Cl free specimens have been reported (Bauer and Berman, 1928). Thus, in these minerals, Cl is not likely to be an essential element.

As observed in Table 1, the z -coordinates of OH (including oxygen and chlorine) take various values, indicating that these ions do not lie in such a flat surface as the OH layer in $\text{Mn}(\text{OH})_2$. In fact the

maximum deviation from the averaged value of the z -coordinates is 0.0749 which corresponds nearly to 0.5\AA . The deviation to such an extent is presumably a result of the misfit between tetrahedral and octahedral-sheets. In this connection, it may be pointed out that no appreciable corrugation of octahedral sheets is observed in trioctahedral micas whose misfit indicators are negative and usually close to zero (Takéuchi, 1965a). The comparatively long distance between Mn1 and OH1 (Table 2) may be considered as due to preferred distribution of Cl atoms over the OH1 sites. However, as far as the three-dimensional difference Fourier maps are concerned, no significant peak is observed at the corresponding locations.

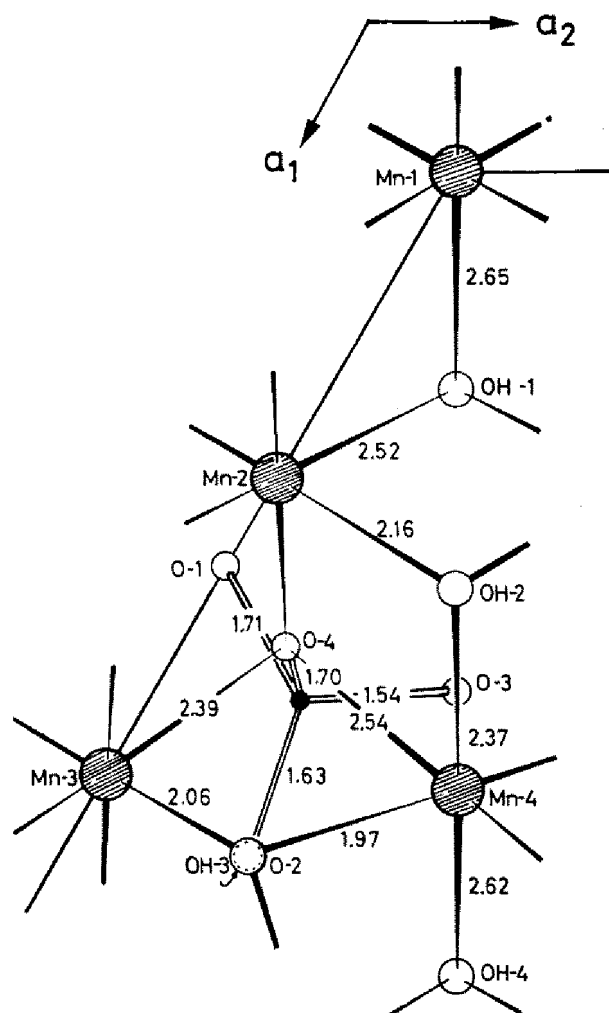


Fig. 6. Bond lengths in manganpyrosmalite.

Polytypism

As explained in the foregoing section, the structure of manganopyrosmalite is regarded as the result of alternate stacking of an Mn octahedral sheet and a tetrahedral sheet. Therefore, like other sheet structures, different modes of sheet stacking are conceivable, each giving a specific polytype.

Among possible polytypes of pyrosmalite, those which retain three-fold axes can be derived in the following way. Firstly, we introduce three symbols t , s and \bar{s} and let them represent respectively a twelve-membered ring, a six-membered ring of tetrahedra whose apices point upwards and that of tetrahedra whose apices point downwards. Then put these symbols in a pair of parentheses and define that the first symbol in the parentheses specifies the type of ring, in a tetrahedral sheet, locating at $(0, 0)$ of the hexagonal plane lattice of pyrosmalite and the second symbol the type of ring at $(2/3, 1/3)$ and the third the one at $(1/3, 2/3)$. Now, since a tetrahedral sheet in a unit cell of the plane lattice consists of each one of the above mentioned rings and their possible locations are $(0, 0)$, $(2/3, 1/3)$ and $(1/3, 2/3)$, any possible orientation of the sheet with respect to the cell axes can be expressed in terms of a specific order of these three symbols. For instance, the silicate sheet shown in Fig. 4 is expressed as $(ts\bar{s})$.

Secondly, for a given silicate sheet, we must consider the possible orientations of successive sheets. Suppose we take a silicate sheet $(ts\bar{s})$, we shall find, as shown in Fig. 7, that there are two possible ways of placing an octahedral sheet on top of the six-membered ring s in the silicate sheet. For case I (Fig. 7), the ring \bar{s} in a new silicate sheet continuous to and above the octahedral sheet is located at $(1/3, 2/3)$, and for case II at $(0, 0)$. In each of these cases, the new silicate sheet may be rotated by $60^\circ \times n$ around the three-fold axis through $(1/3, 2/3)$ for case I, and at $(0, 0)$ for case II. Among these possible

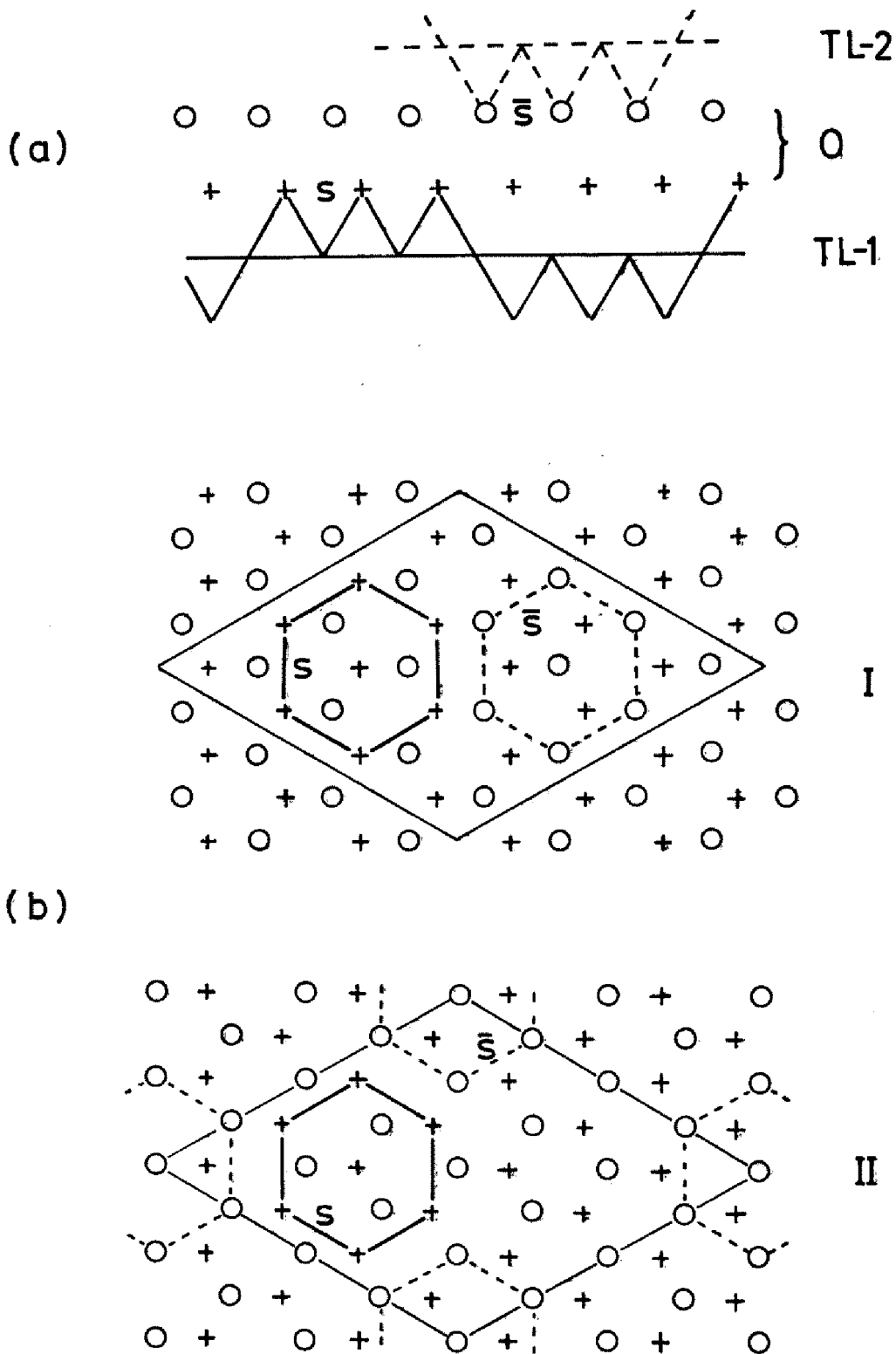


Fig. 7. Relation between tetrahedral sheet and adjacent octahedral sheet. (a) Projection of the tetrahedral and octahedral sheets along [110]. (b) Projection of the octahedral sheet along the *c*-axis. As to the apical hexagon of a ring *s* in a given silicate sheet, TL-1, there are two possible orientations of octahedral sheet, I and II, for each of which the hexagon of a ring *s̄* in the new sheet, TL-2, is indicated. Manganese atoms are not shown.

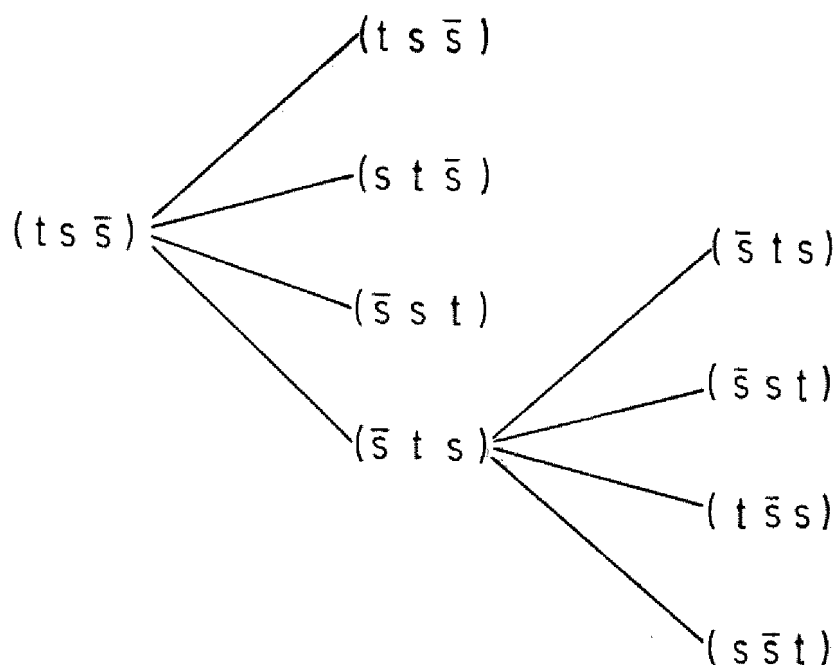


Fig. 8. Diagrammatical illustration of possible sheets adjacent to $(ts\bar{s})$ and to $(\bar{s}ts)$.

rotations, only those of $n=0$ and $n=1$ are discrete, other rotations being equivalent to either one of these two rotations by the symmetry of the sheet. In terms of the sheet notation, the above consideration implies that, for a given sheet $(ts\bar{s})$, the possible adjacent silicate sheet is $(ts\bar{s})$ or $(st\bar{s})$ for case I, and $(\bar{s}st)$ or $(\bar{s}ts)$ for case II. Thus, in general, from the notation of a given sheet, we can formulate two rules to derive those of possible adjacent sheets; (1) when \bar{s} in the given sheet is made invariant, the other two symbols are permutable, and (2) when the positions of \bar{s} and t in the given sheet are interchanged t and s are

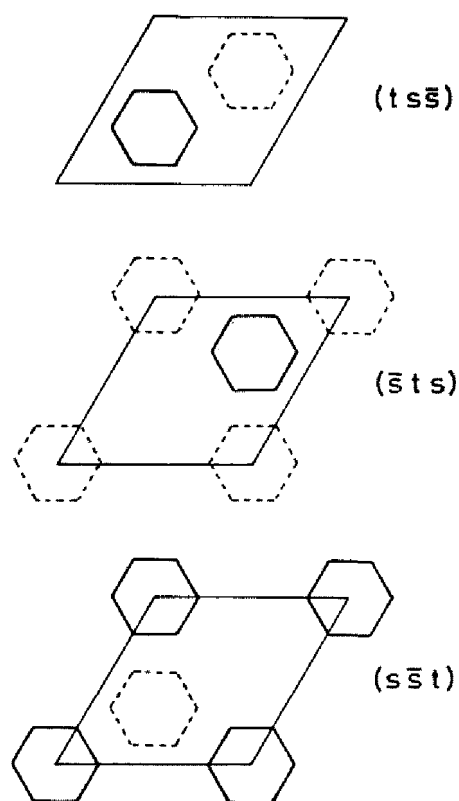


Fig. 9. Sequence of silicate sheets in the three-layer rhombohedral structure.

permutable, \bar{s} at the new position being unchanged. Examples of possible adjacent sheets of $(ts\bar{s})$ and those of $(\bar{s}ts)$ are diagrammatically shown in Fig. 8.

Thus, utilizing the rules given above, we can derive possible sheet sequences which preserve three-fold axes. Some examples are:

$$\begin{aligned} &(ts\bar{s}), (st\bar{s}), (ts\bar{s}), \dots\dots\dots \\ &(ts\bar{s}), (st\bar{s}), (st\bar{s}), (ts\bar{s}), \dots\dots\dots \\ &(ts\bar{s}), (\bar{s}ts), (s\bar{s}t), (ts\bar{s}), \dots\dots\dots \end{aligned}$$

The first example is a two-layer structure having the space group $P3m1$, the second and the third are those of three-layer structures. The space group of the second structure is $P3m1$ and this type of sequence may be extended to n -layer structures, while that of the third is $R3m$. The rhombohedral symmetry is easily recognized in the sequence of notations, three symbols being cyclically permuted. The silicates sheets corresponding to this rhombohedral structure are illustrated in Fig. 9. It is highly probable that the first and the third examples correspond to the structure of schallerite and that of friedelite respectively. According to Frondel and Bauer (1953), the lattice constants of these two mineral species are:

schallerite	friedelite
($P-$)	($R-$)
a 13.43Å	13.40
c 14.31 (= 2×7.155)	21.43 (= 3×7.143)

Though similar considerations will lead us to polytypes of lower symmetry, they will not be discussed here because of their less practical interest.

REFERENCES

- BAUER, L. H. & BERMAN, H. (1928). *Amer. Min.*, 13, 341.
 BUSING, W. R., MARTIN, K. C. & LEVY, H. A. (1962). *A Fortran crystallographic least-squares program, CRNL-TM-305*, Oak Ridge National Laboratory, Oak, Ridge, Tennessee.

- BURNHAM, C. W. (1963). *An IBM 709/7090 computer program for computing transmission factors for crystals of arbitrary shape*. Geophysical Laboratory, Washington, D. C.
- FREED, R. L. & PEACOR, D. R. (1967). *Amer. Min.*, 52, 709.
- FRONDEL, C. & BAUER, L. H. (1953). *Amer. Min.*, 38, 755.
- GOSSNER, B. & MUSSGNUG, F. (1931). *Z. Kristallogr.*, 96, 525.
- IITAKA, Y. (1953). *Acta Cryst.*, 6, 663.
- KASHAEV, A. A. (1968). *Sov. Phys. Crystallography*, 12, 923.
- KUNZE, G. (1956). *Z. Kristallogr.*, 108, 82.
- (1958). *Z. Kristallogr.*, 110, 282.
- MCCONNELL, D. (1954). *Amer. Min.*, 39, 929.
- TAKÉUCHI, Y., KAWADA, I. & SADANAGA, R. (1963). *Acta Cryst.*, 16, A16.
- TAKÉUCHI, Y. (1965a). *Clay and Clay Minerals, 13th Conf.* [1964], Pergamon Press, 1.
- (1965b). To be published.
- TAKEDA, H. & IRIMAZIRI, S. (1967). *Universal program system (1)*, *Cryst. Soc. Japan*, 35 (in Japanese).
- WATANABE, T. & KATO, A. (1957). *Min. Journ.*, 2, 180.
- WATANABE, T., KATO, A. & ITO, J. (1961). *Min. Jour.*, 3, 130.
- WUENSCH, B. J., TAKÉUCHI, Y. & NOWACKI, W. (1966). *Z. Kristallogr.*, 123, 1.

Manuscript received 26 December 1968.